ORNL/TM-2022/2690, PNNL-33374

Monitoring Xenon Capture in Metal Organic Frameworks Using Laser-Induced Breakdown Spectroscopy

Hunter B. Andrews
Praveen K. Thallapally
Alexander J. Robinson

October 2022

OAK RIDGE National Laboratory

ORNL IS MANAGED BY UT-BATTELLE LLC FOR THE US DEPARTMENT OF ENERGY

ORNL/TM-2022/2690, PNNL-33374

Radioisotope Science and Technology Division

MONITORING XENON CAPTURE IN METAL ORGANIC FRAMEWORKS USING LASER-INDUCED BREAKDOWN SPECTROSCOPY

Hunter B. Andrews[1], Praveen K. Thallapally[2], Alexander J. Robinson[2]

[1]Oak Ridge National Laboratory
[2]Pacific Northwest National Laboratory

October 2022

Prepared by
OAK RIDGE NATIONAL LABORATORY
Oak Ridge, TN 37831
managed by
UT-BATTELLE LLC
for the
US DEPARTMENT OF ENERGY
under contract DE-AC05-00OR22725

CONTENTS

LIST OF FIGURES

EXECUTIVE SUMMARY

Molten salt reactor (MSR) operation will result in the transport of fission gases into the headspace of the reactor where in some designs a cover gas will be circulated to remove certain fission products and maintain an inert atmosphere. The cover gas leaving the reactor core is expected to contain both noble and non-noble gases, aerosols, volatile species, tritium, and radionuclides and their daughters. To remove these radioactive gases, it is necessary to develop a robust off-gas system. Various treatment systems must be staged in series to remove the off-gas constituents from the stream before recirculating the gas back to the headspace of the reactor. Several of these treatment systems are being developed under the MSR program.

In this study, a metal organic framework (MOF) was engineered for the capture of xenon, a major contributor to the off-gas source term. The MOF was synthesized and characterized by Pacific Northwest National Laboratory before being sent to Oak Ridge National Laboratory (ORNL) to be tested using a laser spectroscopy sensor. At ORNL, a laser-induced breakdown spectroscopy sensor for noble gas monitoring was developed, optimized, and then used to monitor xenon breakthrough tests benchmarking the high xenon selectivity of the engineered MOF column. This project has demonstrated a cross-laboratory effort to develop novel off-gas treatment and monitoring options.

1. INTRODUCTION

Molten salt reactors (MSRs) are an advanced nuclear reactor design in which the working fluid is a liquid salt and the fuel is either solid or dissolved into the liquid salt. Typically, these salts are either fluorides or chlorides depending on whether the reactor design is a thermal or fast spectrum reactor. MSRs are being pursued because of several inherent advantages over traditional light water reactors, including passive safety features, high exergy, high thermodynamic efficiency, and the potential for greater fissile material utilization.[1,2] This later benefit comes from the capability to perform real-time fission product removal or online reprocessing. Some level of this removal occurs passively as gaseous and volatile fission products leave the salt.

Although this removal is beneficial for reactor neutronics due to fission products with large neutron absorption cross sections leaving the salt, it generates another challenge in that these fission gases need to be properly captured in an off-gas system that acts as a radionuclide boundary and release prevention system. An off-gas system will contain multiple components to treat different aspects of the cover gas coming from an MSR core. These components can include a decay tank for short-lived radioisotopes to decay, a molten hydroxide scrubber for particulate and acidic gas removal, halide, H_2O and O_2 traps, and activated charcoal for noble gas delay.[1,2] There is also the potential for noble gas capture with methods such as cryogenic distillation, which would have a potential commercial value.[1,2] The treated gas stream would then be resupplied to the core as the regenerated cover gas. This concept is illustrated in Figure 1.

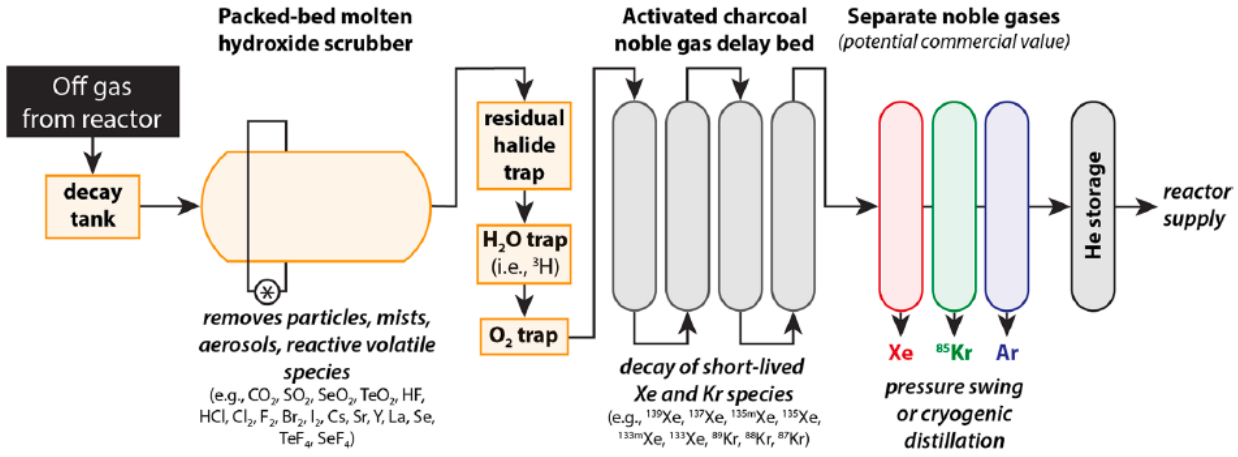

Figure 1. A conceptual MSR off-gas design for fission product removal. This drawing is reproduced with permission from Andrews et al.[2]

The noble gases produced through fission or subsequent decay make up a large contribution of the source term anticipated in the off-gas stream. During the Molten Salt Reactor Experiment (MSRE), activated charcoal was used to hold up these gases long enough for the isotopes to decay. The isotopes of xenon and krypton have a large range of range of half-lives ($t_{½}$) including ^{139}Xe ($t_{½}$ = 39.5 s), ^{137}Xe ($t_{½}$ = 3.83 min), ^{135m}Xe ($t_{½}$ = 15.3 min), ^{135}Xe ($t_{½}$ = 9.1 h), ^{133m}Xe ($t_{½}$ = 2.19 d), ^{133}Xe ($t_{½}$ = 5.25 d), ^{90}Kr ($t_{½}$ = 32.3 s), ^{89}Kr ($t_{½}$ = 3.18 min), ^{88}Kr ($t_{½}$ = 2.84 h), and ^{85}Kr ($t_{½}$ = 10.76 y). The isotopes with half-lives on the scale of hours and days cause the most trouble in terms of treatment and require a significant residence time in the charcoal beds (e.g., 90 days). This requires a large footprint with four to five charcoal beds 6–9 feet in diameter, and 50 feet in length. Additionally, because of the heat production from radioactive decay, these beds could pose a potential fire hazard if any oxygen remains in the stream.

An alternative technology to charcoal delay beds is metal organic frameworks (MOFs). MOFs are highly porous crystalline materials composed of metal ions linked by organic molecules. The combination of metal ions and organic linker molecules allows these materials to be engineered for specific gas selectivity. These porous structures have several advantages compared with charcoal delay beds, including a significant cost reduction from a higher selectivity and capacity, smaller size, and posing no fire hazard. Additionally, xenon and krypton can be captured in separate steps, which might permit the gases to be sold for their commercial value. These engineered MOFs are currently being developed for MSR gas capture by a team at Pacific Northwest National Laboratories (PNNL).

In addition to the need to develop more efficient off-gas treatment components, there is a need to develop sensors to be used in-line with these components that can monitor species' concentrations. The mixed gas and particulate stream, anticipated radiation field, and breadth of analytes makes monitoring an MSR off-gas system a challenge for traditional approaches. Currently, there is an ongoing collaborative effort between PNNL and Oak Ridge National Laboratory (ORNL) to develop optical spectroscopy sensors for monitoring an MSR off-gas system. To accomplish this, PNNL is focused on molecular approaches (e.g., Raman spectroscopy) and ORNL is focused on elemental approaches (e.g., laser-induced breakdown spectroscopy [LIBS]). Optical spectroscopy is ideal for online monitoring because it is sensitive to a large array of analytes, can be deployed remotely using optical fibers, and can monitor both stable and radioactive species. LIBS has recently been demonstrated to be capable of monitoring both aerosolized species and noble gases in real time.[3,4] A sensor such as this would be a valuable tool to be coupled with noble gas treatment components being evaluated on an MSR off-gas testbed.

The goal of this project was twofold: (1) develop sorbents and fabricate them into an engineered form to capture noble gases at or near room temperature and (2), after characterizing the sorbent an optical spectroscopy gas sensor was integrated to monitor noble gas capture. These activities demonstrated the use of optical spectroscopy coupled with sorbent materials to capture and monitor the noble gases in real time and resulted in an engineered gas treatment testbed for future component development and evaluation.

2. METAL ORGANIC FRAMEWORK SYNTHESIS

2.1 BACKGROUND

MSRs are being investigated as an advanced nuclear power technology for deployment in the next decade.[1, 2] Depending on the molten salt fuel mixture, a variety of radioactive or nonradioactive radionuclides can be released into the headspace of the reactor. Typical off-gas composition during the MSRE in the 1960s included iodine, noble gases (xenon and krypton), halides, hydrogen, water, nitrogen, oxygen, and reactive gases (e.g., chlorine and fluorine). The concentration of these components in the off-gas system varied and was dependent on the thermochemical and thermophysical properties of the molten salt and its movement through the reactor. The main focus of our work is on noble gases because they are produced at high yield and may be commercially valuable. The radionuclides generated continuously during reactor operation and from demand-driven salt cleanup must be captured to meet public safety as defined by regulatory limits. Today's most mature capture technology for volatile species with short half-lives is based on passing the off-gas stream through delay beds containing activated carbon to adsorb and decay (radionuclides) followed by cryogenic distillation or pressure swing adsorption to separate xenon and krypton. The separated xenon and krypton are then stored at a higher pressure in a stainless-steel canister. Though these existing technologies have been shown to exhibit acceptable adsorption capacity towards xenon and krypton, their sorption performance is significantly reduced in the presence of other competing gases. Moreover, installing and operating a cryogenic process to separate noble gases is expensive and has long-term cost implications because of high energy demands.

To overcome the cryogenic distillation approach, PNNL developed a novel class of porous materials including zeolites[5], porous organic cages[6], covalent organic frameworks[7], porous organic polymers[8], and MOFs for selective removal of xenon and krypton at near room temperature. Among all the MOFs tested, the calcium-based MOF, CaSDB (SDB = 4,4'-sulfonyldibenzoate, with a pore diameter of 4.5 Å was shown to outperform all the materials tested at room temperature (Figure 2).[9] Because of the high polarizability of Xe, the majority of the MOFs capture Xe selectively over other gases, including Kr. Therefore, we have demonstrated a two-column approach using CaSDB where bed 1 selectively removes Xe at room temperature from a gas mixture consisting of 1,300 ppm Xe, 130 ppm Kr, 300 ppm CO_2, 0.9% Ar, 78.2% N_2, and 21% O_2. The off-gas mixture (without xenon) exiting bed 1 was passed through bed 2, containing CaSDB at room temperature, to remove krypton. Further, the xenon and krypton adsorption capacity were not affected even by 48% relative humidity, although humidity should not be an issue with MSR off-gases.[10] Similarly, MOFs can be modified to target gases of interest in MSRs, capturing volatile fission products and nonradioactive gases evolved during MSR operations. ORNL is developing advanced online instrumentation to monitor the off-gases released during reactor operation.[3,4] As part of this collaboration, PNNL scaled up the MOF material and shipped it to ORNL. The objective was to evaluate the MOF performance using LIBS to monitor the noble gases released in real time.

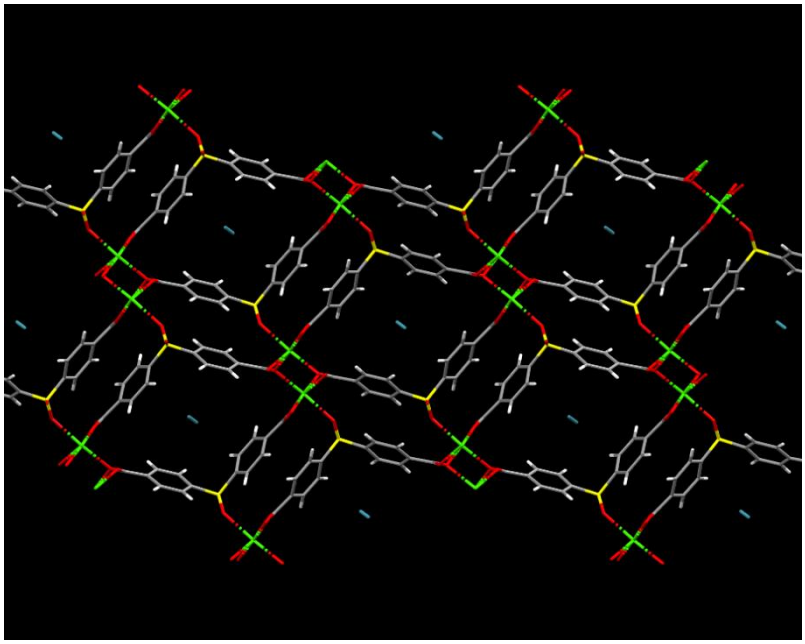

Figure 2. Crystal structure of CaSDB with pores (blue) occupied with gas molecules.

2.2 SYNTHESIS AND FABRICATION OF CaSBD

The CaSDB was synthesized under solvothermal conditions from a stoichiometric solution of 4,4' sulfonyldibenzoic acid (SDB), and $CaCl_2 \bullet 2H_2O$, modified from published procedures.[11] A 2 L glass liner was charged with 1.0 L of EtOH, SDB (16.45 g, 53.7 mmol), and $CaCl_2 \bullet 2H_2O$, (8.48 g, 57.7 mmol) then sealed in a 2 L stainless steel Parr reactor. The vessel was heated to 180°C for 48 h to yield an off-white crystalline powder. The powder was washed with acetone (3 × 35 mL) and collected by filtration. Figure 3 shows the 2 L Parr reactor used in the MOF scale-up. To prepare engineered particles of CaSDB, powdered CaSDB was packed into a silicon tube and pressed at 2,000 psi (13.8 MPa) for 3 min using an isostatic press (Figure 3) to obtain CaSDB pellets. The pellets were carefully broken up, and the

fragments were sieved for 600–850 μm size particles. X-ray diffraction (XRD) measurements were used to analyze the phase composition and structure of CaSDB powder and the CaSDB engineered particles. The sample was placed in a powder sample holder under ambient conditions, and an XRD pattern was collected continuously using CuKα1 radiation (λ = 1.54056, 2θ range from 5°–40°). The bulk sample XRD signal is identical to the simulated XRD signal, suggesting the phase purity of the CaSDB (Figure 4).

Figure 3. Two-liter Parr reactor and isostatic press used to fabricate the synthesized MOF powder into engineered particles.

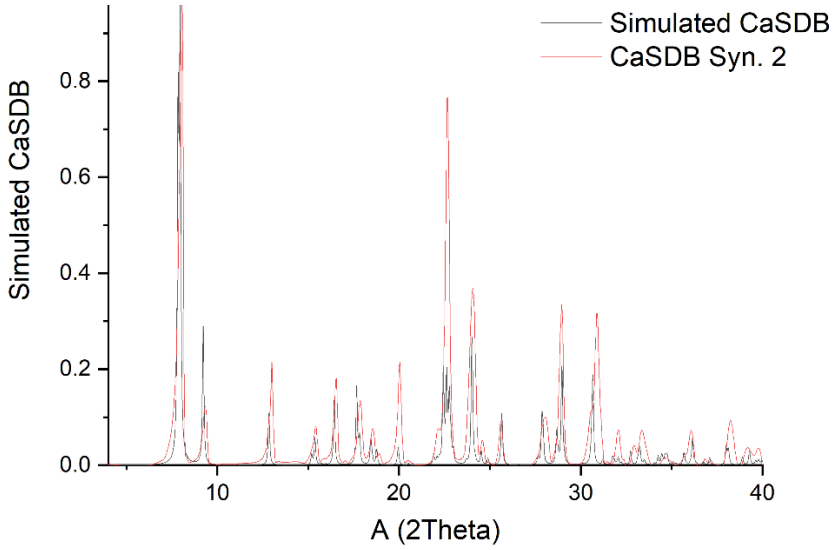

Figure 4. Simulated and experimental powder X-ray diffraction of synthesized CaSDB powder.

To further evaluate the CaSDB purity and structural integrity, single component gas adsorption analysis was performed using an in-house gas adsorption analyzer. The sample was activated at 100°C under vacuum at a rate of 5°C min^{-1} on the outgassing side of the instrument. The sample was then cooled to room temperature, and the dry mass was measured. The experimental temperature of 25°C was maintained by a water bath. The pressure points were set beforehand using the software. Volumetric changes, resulting from adsorption at each pressure step, were plotted against the pressure. The pure-component xenon adsorption isotherms at room temperature were performed to demonstrate the purity of the MOF powder and engineered particles. Both forms of MOF samples saturate quickly (at 0.2 bar), which is indicative of a strong framework-xenon interaction. At room temperature and 1 bar, the MOF adsorbs 1.3 mmol g^{-1} of xenon; while under the same conditions, krypton adsorption is 0.8 mmol g^{-1}. However, the engineered particles have a slightly lower xenon and krypton adsorption capacity at all the pressure points (Figure 5). The XRD coupled with pure component gas adsorption data on the CaSDB MOF suggest the phase purity of the synthesized material is adequate.

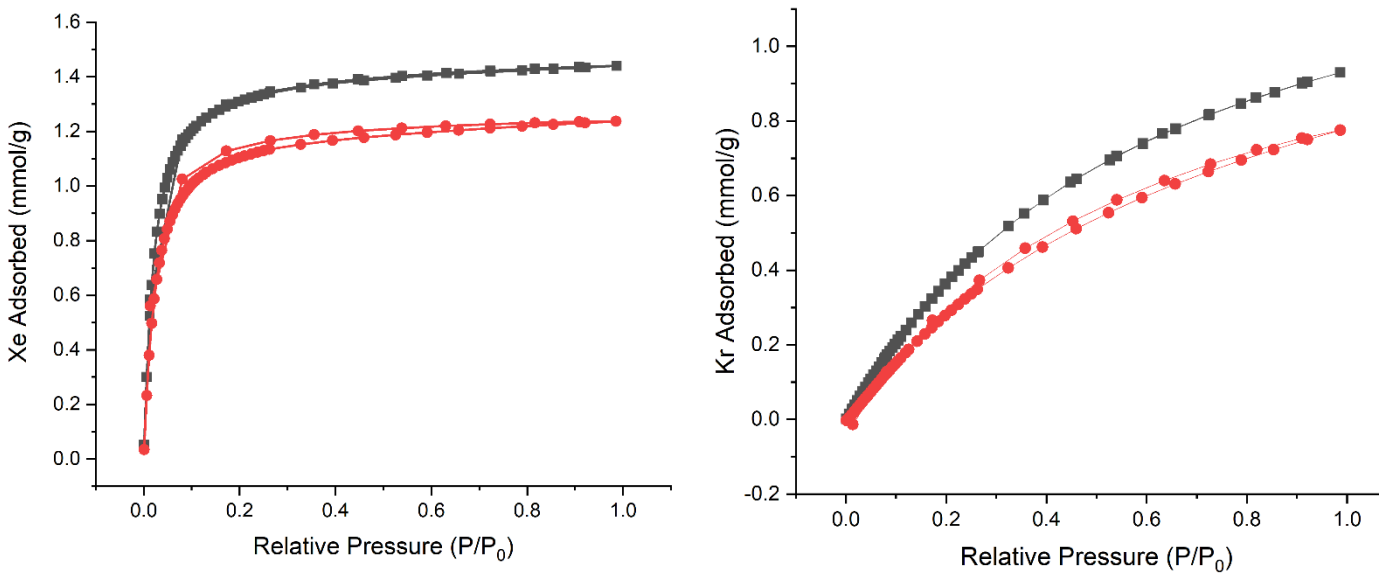

Figure 5. Noble gas adsorption and desorption at room temperature using CaSDB MOF powder (black) and engineered particles (red).

As part of a Gateway for Accelerated Innovation in Nuclear (GAIN) voucher, PNNL compared the performance of CaSDB MOF to that of carbon filters produced by NUCON international (standard material) using simulated off-gas composition present in MSRs.[12] Single column breakthrough experiments were performed at different temperatures, activation conditions, flow rates, and off-gas compositions to optimize the xenon capacity at the breakthrough point and at saturation. The xenon loading in CaSDB MOF was compared with standard solid sorbent (NUCON carbon) under identical conditions. Based on the single column experiments, CaSDB MOF outperforms the NUCON carbon at all the temperatures and reduces the mass (to as little as 55%) of sorbent needed to achieve the same performance as carbon. The bed volume is also reduced, down to 48% of that of NUCON carbon, when the MOF is used. These results clearly demonstrate improvement in the amount of adsorbent needed and show a reduction in bed volume compared with traditional sorbent material.

To evaluate this MOF in-line with LIBS, ~1 gram of engineered particles was packed in a stainless-steel tube and sent to ORNL for further evaluation.

3. LASER-INDUCED BREAKDOWN SPECTROSCOPY ANALYSIS

LIBS is performed by focusing a pulsed laser beam into a point where its energy density is great enough to cause gaseous breakdown or ablate a solid material to then form a plasma. The generated plasma will rapidly cool, and as it de-excites, characteristic photoemissions occur. These can be observed and measured using optical lenses, fiber-optic cables, and a spectrometer. The spectrometer passes the light through a small slit and then diffracts the light using precise gratings onto a detector, which converts the photons to a digital spectrum. The resultant spectrum ranges from the ultraviolet up to the near infrared region (e.g., 200–1000 nm).

Our recent work has demonstrated the capability to monitor aerosolized species including Rb, Cs, Gd, Nd, and Sm at very low concentrations in real time.[3,4] These aerosol species were also monitored along with noble gases (xenon and krypton), offering a more representative study to an MSR off-gas system.[4] These

studies operated at a larger scale than the current study, with flow rates on the order of 2 L min^{-1}. Because of this difference in scale, a new experimental LIBS setup was required for testing the MOF performance.

3.1 EXPERIMENTAL SETUP

A three-way gas manifold system was configured with mass flow controllers (Sierra, SmartTrak100) calibrated for Ar, Kr, and Xe gas flows up to 3 mL min^{-1}. Each line was attached to compressed cylinders with pure source gasses (AirGas, 99.99%). Following the junction after the mass flow meters, the gas line was plumbed into a laser enclosure for LIBS measurements. The gas line was delivered to the sampling point using a pipette tip as a nozzle aimed toward the surface of an aluminum substrate. A 532 nm Nd:YAG laser (Big Sky Laser, Ultra50) was fired and focused down onto the aluminum substrate. The substrate was used to ensure breakdown occurred at a repeatable position. The height of the aluminum substrate was aligned with the laser focal point using a Keyence laser to measure distance. The plasma light was collected at ~45° from the laser pulse and was routed to the spectrometer using a 2 m fiber-optic cable (Avantes, FC-UV200). An echelle-type spectrometer (Catalina Scientific, EMU-120/65) was used along with an electron multiplying charged-coupled device (Raptor Photonics, Falcon Blue) and a pulse generator for external triggering (Quantum Composers, Model 9214). The spectrometer was wavelength calibrated using a Hg:Ar lamp (StellarNet Inc, SL2). A diagram of the planned experimental setup is shown in Figure 6. A photo collected during a measurement on the built system is shown in Figure 7.

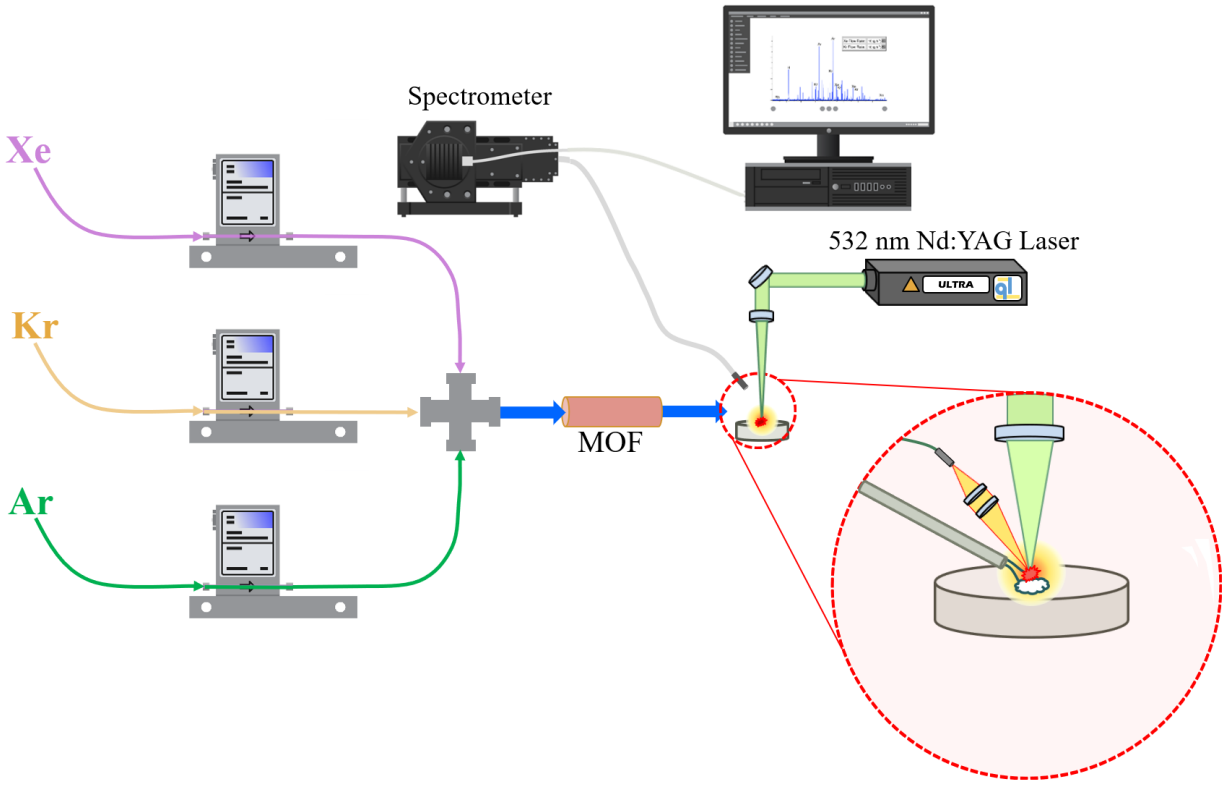

Figure 6. Experimental schematic for LIBS gas analysis with MOF filter.

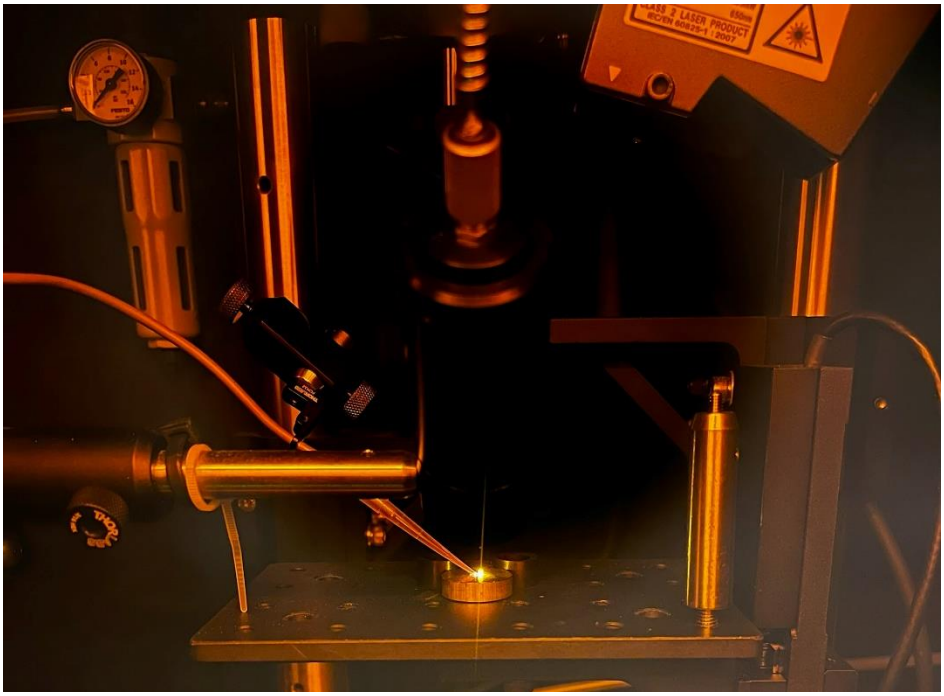

Figure 7. LIBS plasma formation on surface of aluminum substrate with gas nozzle diretly adjacent. The applied 532 nm laser pulse is fired directly downward onto the substrate, and the plasma is collected using the optics shown in the center of the photo.

3.2 PRELIMINARY TESTING

Before any system optimization, the LIBS system and mass flow controllers were tested with pure gas streams to ensure adequate performance. This step also provided a convenient opportunity to identify the emission peaks for the species of interest (e.g., Ar, Kr, and Xe). The pure spectra for each gas species are shown overlaid in Figure 8. Over the 140 nm wavelength range shown are several unique peaks for argon and krypton. Xenon, however, has far fewer strong emissions, and several of them are convoluted with other species' emissions. Fortunately, the four strongest xenon emission peaks at 823.15, 834.67, 875.56, and 881.95 nm have little interference or have a far larger relative intensity than their interferent peaks. A handful of other emission peaks of relevant species are seen outside the spectral range plotted in Figure 8.

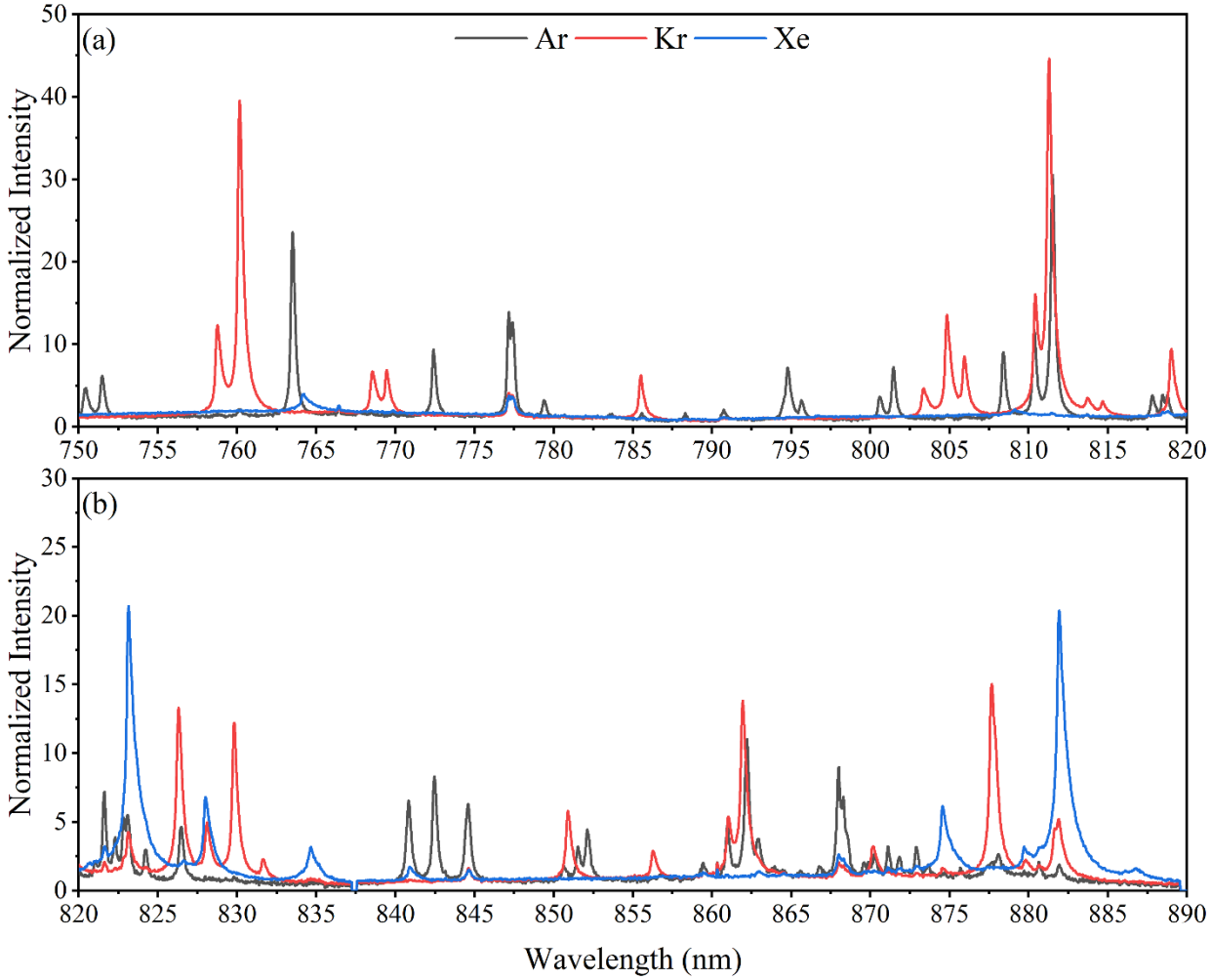

Figure 8. LIBS spectra of pure Ar, Kr, and Xe gases overlaid for peak identification. The spectra shown are 100 shot averages taken at flow rates of ~30 mL min^{-1}.

LIBS measurements are subject to the acquisition settings used when forming the plasma and observing it. These settings include spectrometer delay time, spectrometer exposure time, laser energy, and the number of shots used. Typically, these parameters are optimized by investigating the signal response to changes through tracking the signal-to-background ratio (SBR). The SBR is defined in Equation 1. The system settings were optimized using the pure argon gas to conserve the noble gas stocks. In particular, the 763.5 nm argon (I) peak was monitored as it had a similar spectral response to the krypton and xenon peaks.

$$\mathrm{SBR} = \frac{\text{Emission peak intensity}}{\text{Nearby baseline intensity}} \quad . \tag{1}$$

First, the spectrometer gating was optimized. The spectrometer gate delay is the time between the laser pulse firing and the spectrometer initiating light collection. The spectrometer exposure time is the length of time that the spectrometer continues to measure light following the gate delay. The spectrometer used in this study did not have an internal shutter, meaning there was an effective minimal exposure time. In this case, even if the system were set to a lower exposure time the detector would experience frame smearing, which can lead to false peaks and increased background levels. The results of the spectrometer

gating optimization are shown in Figure 9. The minimal exposure time was determined to be 200 µs. As shown in Figure 9 (left), the SBR values show irregular trends at 50 and 100 µs, but the trend becomes linear at 200 µs. This minimum exposure time was used moving forward to enable data collection as rapidly as possible. As for gate delay, Figure 9 (right) shows the response of the 763.5 nm argon (I) peak as the delay is varied. As the delay time is increased, the peak grows in intensity and the background levels fall. The background levels fall as the result of having less white light from the plasma continuum existing later into the plasma lifetime. The optimal gate delay was determined to be 0.5 µs.

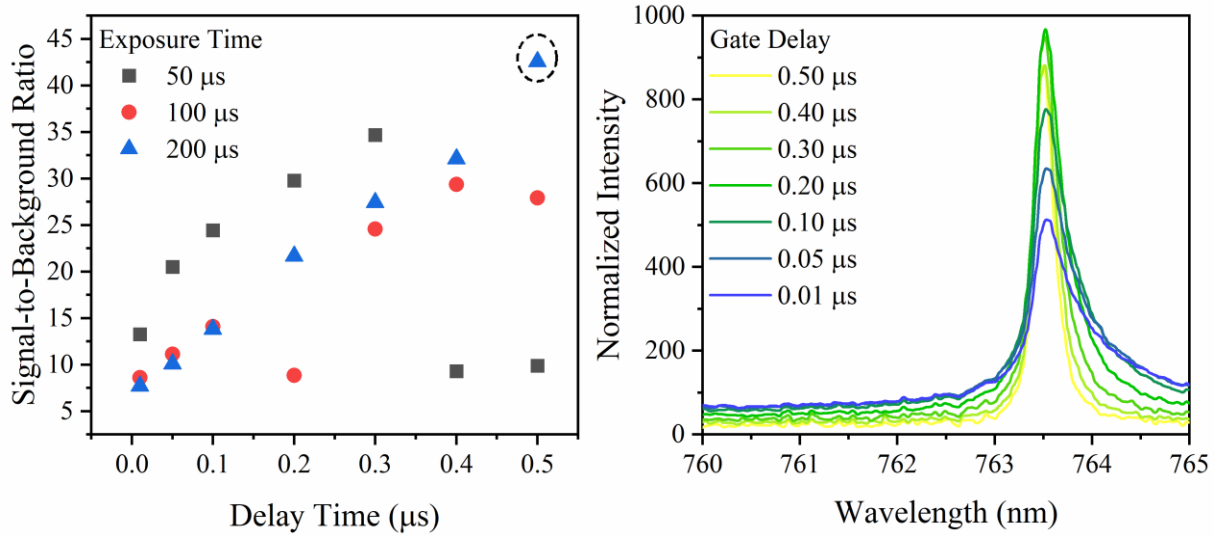

Figure 9. The 763.5 nm argon (I) emission peak response as the spectrometer gate delay was modified and the exposure time held constant at 200 µs (left) and the corresponding SBR values for the peak over the gating parameters investigated (right). The selected settings are indicated by the circled data point (delay = 0.5 µs, and exposure time = 200 µs).

Following the spectrometer gating optimization, the laser pulse energy was investigated. Laser pulse energy and signal intensity are directly linked through the ablation process. The laser energy affects the ablation and plasma formation, directly impacting the peak plasma temperature and electron density. Plasma temperature and electron density affect the relative ratios of the species' ionization levels in the plasma, as well as the transition rates (i.e., intensities) of species. The laser used in this study had an upper energy limit of 50 mJ pulse^{-1}. The laser energy was varied from 10% to 100% using the toggle on the power unit. The laser could barely form a plasma at 10% energy, but above this level an adequate plasma was always formed. The response of the 763.5 nm argon (I) peak to changes in the laser energy are shown on the left of Figure 10.

To optimize the energy setting, not only was the SBR taken into consideration but also the signal intensity itself was given weight, as shown on the right of Figure 10. If only the SBR is considered, then 10% energy would be the optimal value; however, as mentioned previously, plasma formation was an issue at this level. The SBR at 10% energy is so large purely because of there being nearly no background intensity levels. To determine the optimal energy, the tested settings were given percentile ranks for their SBR and intensity values. These ranks were then multiplied by one another to provide an overall score, which indicated 20% energy to be the optimal balance of high SBR and large signal intensity. This corresponds to a pulse energy of approximately 10 mJ.

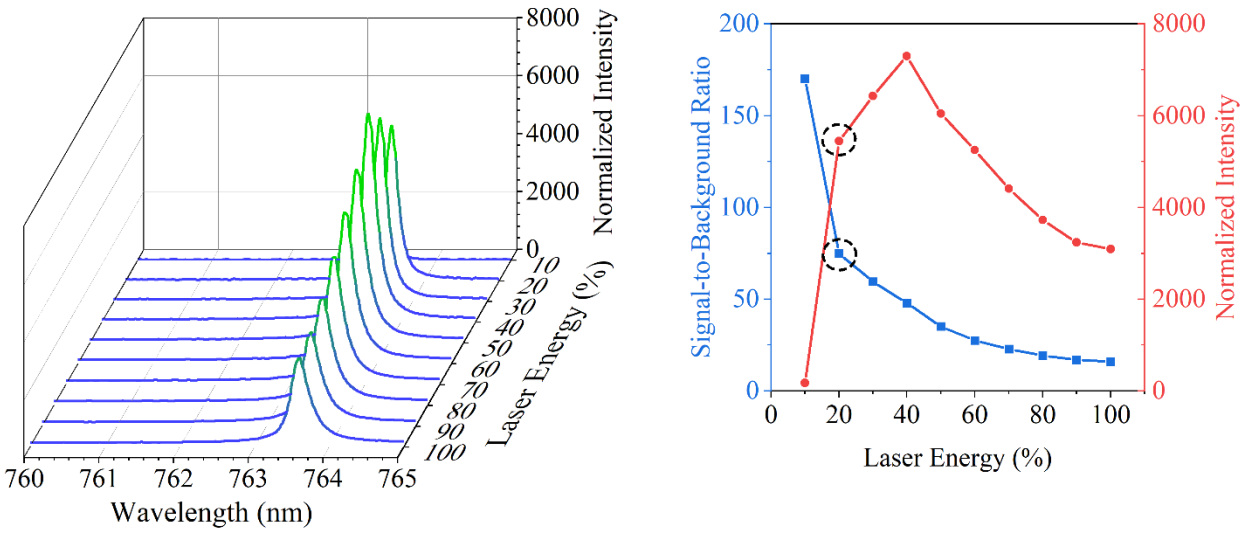

Figure 10. The 763.5 nm argon (I) emission peak response as the laser energy was modified (left) and the corresponding SBR and peak intensity values (right). The optimal energy level is indicated by the circled data points (energy = 20%).

With the acquisition settings optimized, the next step was to measure the spectra over a range of xenon concentrations to develop a calibration curve. Xenon and argon flow rates were adjusted to test gas mixtures ranging from ~1,000–2,500 ppm xenon. Ten minutes was allowed to pass between changing the gas flow rates to allow the system to equalize and allow the new gas ratio to reach the measurement point. A total of 300 spectra were collected at each gas ratio.

Figure 11 shows four major xenon peaks' response to the change in xenon concentration. The spectra shown have been normalized to the 763.5 nm argon (I) peak to account for variation. The 823.1 and 881.9 nm neutral xenon emission peaks show the largest response. Based on this, a univariate calibration model was built using the 881.9 nm xenon (I) peak areas. The peak areas were calculated by fitting the spectral region with a Voigt function. A Voigt function is a combination of Gaussian and Lorentzian functions that has been found to fit the emission profile of LIBS peaks well. The produced calibration curve is shown in Figure 12(a). The univariate model showed a good fit with a coefficient of determination of 0.84. These peak areas were used to approximate the limits of detection (LOD) and the limits of quantification (LOQ) of the LIBS setups using Equations 2 and 3:

$$LOD = \frac{3 \cdot s}{m}, \text{and} \tag{2}$$

$$LOQ = \frac{10 \cdot s}{m}, \tag{3}$$

where s refers to the standard deviation, or noise, of the blank and m is the slope of the calibration curve.[13] The LOD and LOQ for xenon were calculated to be 58.2 and 194 ppm, respectively. These metrics demonstrated that the LIBS system was adequate for testing the xenon capture of the provided MOF.

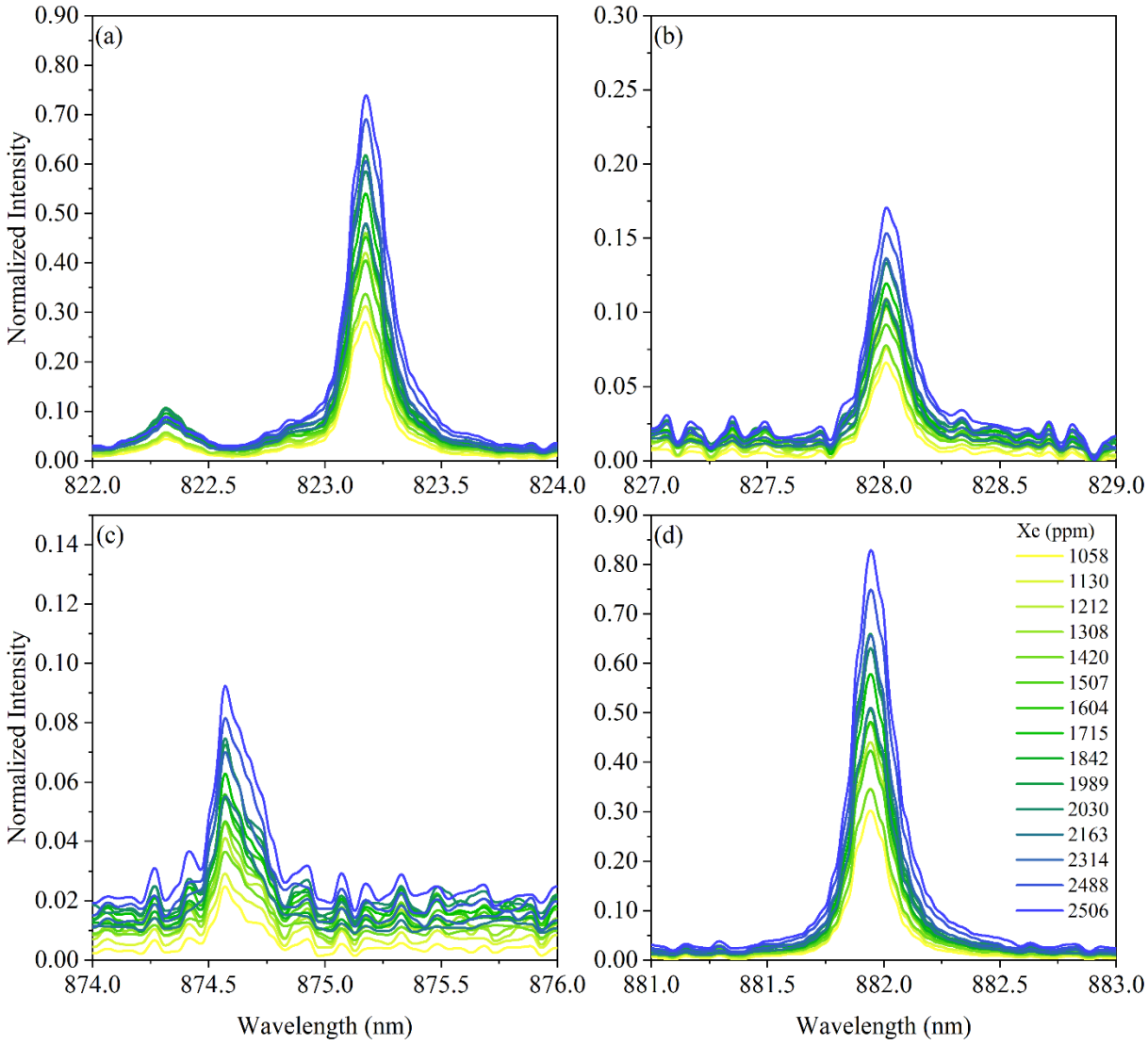

Figure 11. Intensity response of the unconvoluted xenon peaks as the xenon-to-argon mass flow rate ratio is modified. Each spectrum shown is the average of 300 shots and is normalized to the 763.5 nm argon (I) peak.

In addition to the univariate model, a multivariate xenon model was built using partial least squares (PLS) regression. PLS has been demonstrated to provide robust multivariate models that can cope with matrix effects better than univariate models by regressing multiple peaks. The model was set up to use two latent variables that, upon investigation of their loadings, appeared to model the xenon emissions and then the argon emissions. The model was constructed using 70% of the collected spectra and was tested with the remaining 30%. The model predicted the xenon concentrations in the test set well, with a root-mean-squared error of prediction of 88.6 ppm. A parity plot comparing the known to predicted xenon concentrations of the test set is shown in Figure 12(b).

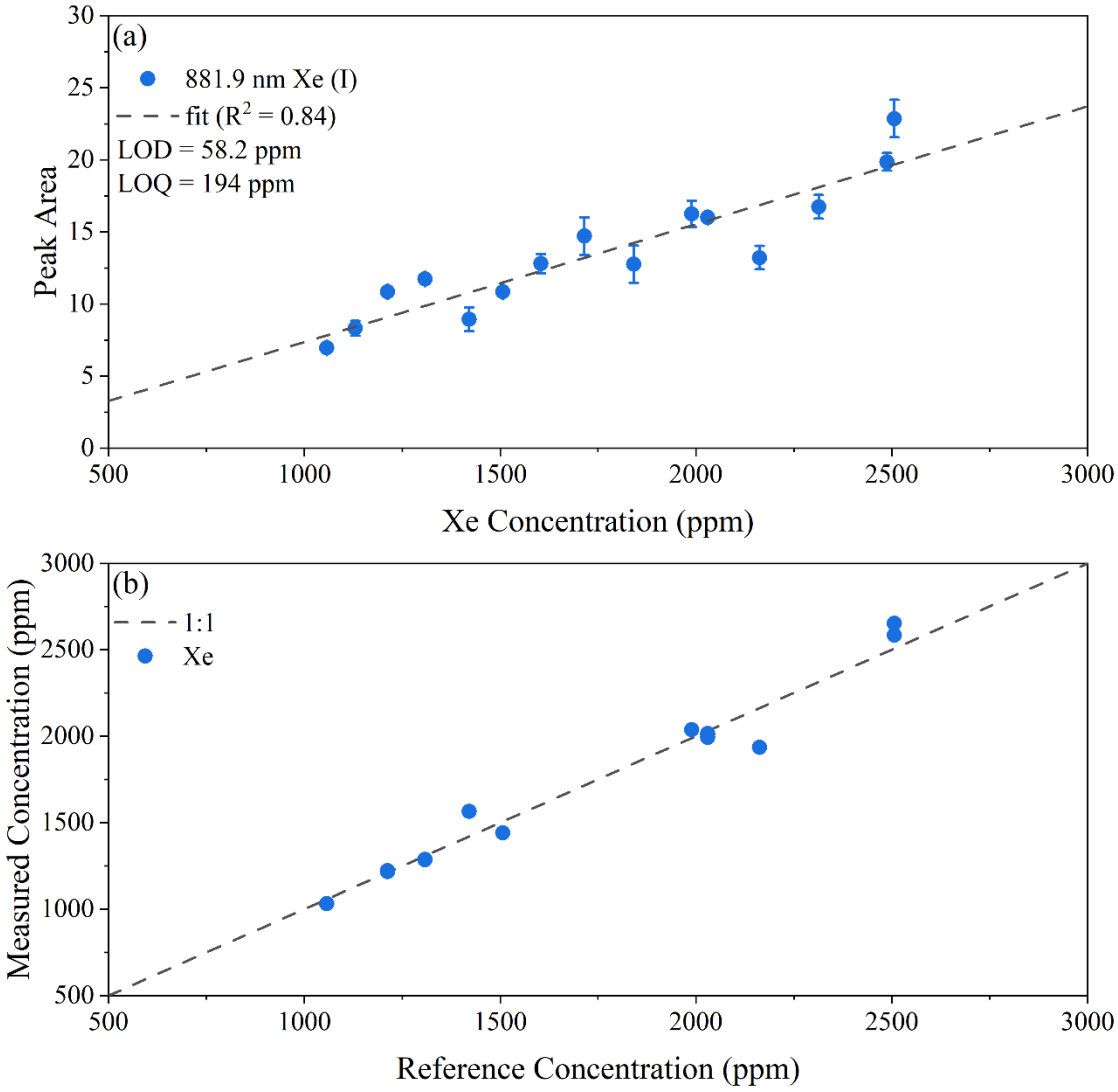

Figure 12. (a) Univariate calibration curve produced from the 881.9 nm xenon (I) peak areas and (b) a comparison of reference and measured xenon concentrations using a 2 latent variable PLS model.

3.3 REAL-TIME MOF TESTS

Following the system optimization and preliminary gas testing, a breakthrough test to investigate xenon capture by the engineered MOF was performed with the LIBS sensor. The MOF, as prepared by PNNL, was activated in a vacuum oven at 100°C for 12 hours to remove any absorbed gases. The MOF was then connected into the test system. The mass flow controllers were used to adjust the gas stream composition to ~1,068 ppm xenon and 1,019 ppm krypton, with the balance being argon, at a flow rate of 28 mL min^{-1}. While bypassing the MOF, this gas stream ran for 10 min to establish an equilibrium. Then the LIBS instrument was initiated and run for 2 min before the bypass was switched to direct gas flow through the MOF column. This time was recorded and is referred to as t_0. The LIBS measurements continued until the 881.9 nm xenon (I) peak was present in the spectra. The laser was operated at 2 Hz.

After 33.5 min of data collection, the test was concluded. The spectra were processed by normalizing them to the 763.5 nm argon (I) line and then calculating the 881.9 nm xenon (I) and 760.1 nm krypton (I)

peak intensities. The signal intensities at 2 Hz had large variances, so 40 shot accumulates were used to provide a more stable signal while still maintaining a decent temporal resolution (20 s spectrum^{-1}). The normalized signal intensities are plotted against time in Figure 13. It can be seen that upon turning the bypass off at t = 2 min the noble gas intensities fall rapidly. After this time, the krypton and xenon levels fall rapidly as the remaining gas between the MOF and LIBS sensor is exhausted. The krypton passes through the MOF with little absorption at a breakthrough time of 0.8 min. Conversely, xenon is captured by the MOF, as desired, with a breakthrough time of 13.3 min. Using the gas composition, MOF mass (nominally 1 g), and breakthrough times, the MOF selectivity can be calculated as

$$S_{Xe/Kr} = \frac{x_{Xe}/y_{Xe}}{x_{Kr}/y_{Kr}} \ , \tag{4}$$

where x corresponds to the mole fraction absorbed by the MOF and y corresponds to the mole fraction in the bulk gas.[14] The selectivity of the engineered CaSDB MOF for xenon relative to krypton was estimated to be 17 based on these breakthrough times. Note, this selectivity value and any associated capacity calculations in this case are based on a proof-of-principal study using LIBS monitoring and should not be used for MOF design considerations at this point.

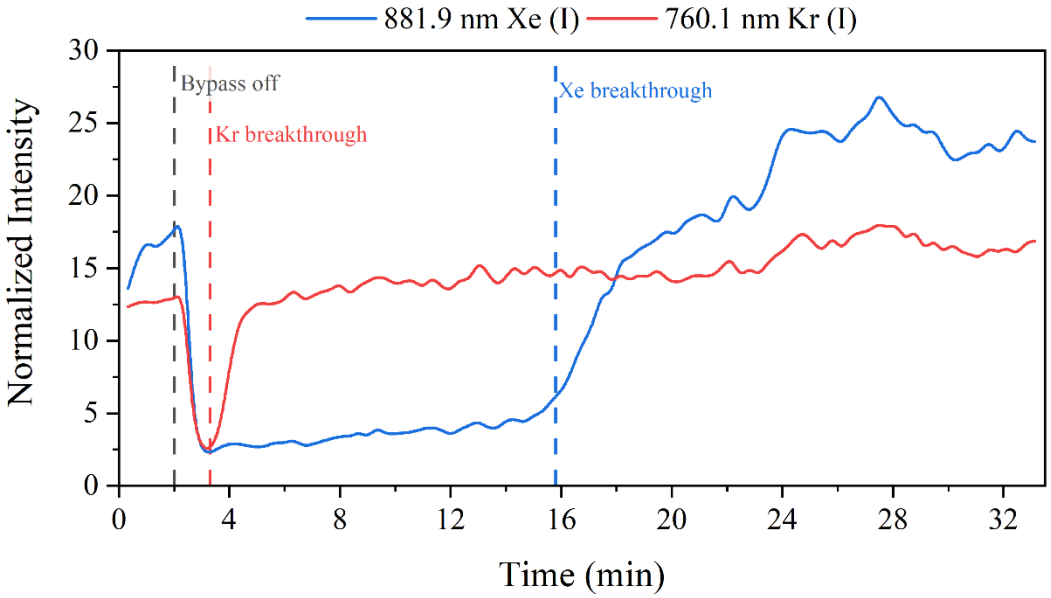

Figure 13. Xenon and krypton signal intensities before and during MOF breakthrough tests. The engineered MOF shows a high selectivity towards xenon, as designed.

4. CONCLUSION

MSRs offer many benefits as an advanced nuclear reactor design, but they also offer complex challenges. One key difference from traditional light water reactors is the liquid fuel in certain MSR designs. In these reactor concepts, fission gases and other volatile species would evolve from the salt, necessitating a gas treatment system. Treatment components for such systems are actively being developed to optimize performance. MOFs are one of these advanced treatment components being researched for gas capture.

In this study, an engineered MOF was synthesized and packed into a column at PNNL and then sent to ORNL to undergo breakthrough testing using a laser sensor to monitor for real-time changes in gas composition. These tests successfully demonstrated both the MOF column's high selectivity towards xenon and the benefits of optical spectroscopy for real-time monitoring. The testing framework established under this project permits future testing of such engineered filters with precisely mixed gas streams and LIBS monitoring. Some of this future work could involve different MOF compositions, investigating temperature effects of gas capture, or scaling tests where large columns and more concentrated gases are tested.

5. ACKNOWLEDGMENTS

The authors would like to thank Patricia Paviet (PNNL), Joanna McFarlane (ORNL), and Brian Robinson (US Department of Energy Headquarters) for their helpful discussion and support. This work was funded by the US Department of Energy's Office of Nuclear Energy, Advanced Reactor Development Program, Molten Salt Reactor Program.

6. REFERENCES

1. Riley, B. J.; McFarlane, J.; DelCul, G. D.; Vienna, J. D.; Contescu, C. I.; Forsberg, C. W., Molten Salt Reactor Waste and Effluent Management Strategies: a Review. *Nucl Eng Des* **2019,** *345*, 94-109.
2. Andrews, H. B.; McFarlane, J.; Chapel, A. S.; Ezell, N. D. B.; Holcomb, D. E.; de Wet, D.; Greenwood, M. S.; Myhre, K. G.; Bryan, S. A.; Lines, A.; Riley, B. J.; Felmy, H. M.; Humrickhouse, P. W., Review of Molten Salt Reactor Off-Gas Management Considerations. *Nucl Eng Des* **2021,** *385*.
3. Andrews, H. B., Myhre, K. G., Quantification of Lanthanides in a Molten Salt Reactor Surrogate Off-Gas Stream Using Laser-Induced Breakdown Spectroscopy. *Applied Spectroscopy* **2022**, 76(8), 877-886.
4. Andrews, H. B., McFarlane, J., Myhre, K. G., Monitoring Noble Gases (Xe and Kr) and Aerosols (Cs and Rb) in a Molten Salt Reactor Surrogate Off-Gas Stream Using Laser-Induced Breakdown Spectroscopy (LIBS). *Applied Spectroscopy* **2022**, 76(8), 988-997.
5. Feng, X. H.; Zong, Z. W.; Elsaidi, S. K.; Jasinski, J. B.; Krishna, R.; Thallapally, P. K.; Carreon, M. A., Kr/Xe Separation over a Chabazite Zeolite Membrane. *J Am Chem Soc* **2016,** *138* (31), 9791-9794.
6. Chen, L.; Reiss, P. S.; Chong, S. Y.; Holden, D.; Jelfs, K. E.; Hasell, T.; Little, M. A.; Kewley, A.; Briggs, M. E.; Stephenson, A.; Thomas, K. M.; Armstrong, J. A.; Bell, J.; Busto, J.; Noel, R.; Liu, J.; Strachan, D. M.; Thallapally, P. K.; Cooper, A. I., Separation of rare gases and chiral molecules by selective binding in porous organic cages. *Nat Mater* **2014,** *13* (10), 954-960.
7. Banerjee, D.; Simon, C. M.; Elsaidi, S. K.; Haranczyk, M.; Thallapally, P. K., Xenon Gas Separation and Storage Using Metal-Organic Frameworks. *Chem-Us* **2018,** *4* (3), 466-494.
8. Chakraborty, D.; Nandi, S.; Sinnwell, M. A.; Liu, J.; Kushwaha, R.; Thallapally, P. K.; Vaidhyanathan, R., Hyper-Cross-linked Porous Organic Frameworks with Ultramicropores for Selective Xenon Capture. *Acs Appl Mater Inter* **2019,** *11* (14), 13279-13284.
9. Sun, Q.; Zhu, L.; Aguila, B.; Thallapally, P. K.; Xu, C.; Chen, J.; Wang, S.; Rogers, D.; Ma, S. Q., Optimizing radionuclide sequestration in anion nanotraps with record pertechnetate sorption. *Nat Commun* **2019,** *10*.
10. Liu, J.; Fernandez, C. A.; Martin, P. F.; Thallapally, P. K.; Strachan, D. M., A Two-Column Method for the Separation of Kr and Xe from Process Off-Gases. *Ind Eng Chem Res* **2014,** *53* (32), 12893-12899.
11. Banerjee, D.; Simon, C. M.; Plonka, A. M.; Motkuri, R. K.; Liu, J.; Chen, X. Y.; Smit, B.; Parise, J. B.; Haranczyk, M.; Thallapally, P. K., Metal-organic framework with optimally selective xenon adsorption and separation. *Nat Commun* **2016,** *7*.

12. Thallapally, P. K., Robinson, A. J., Zbib, A., Riley, B. J., Chong, S., Liu, J., Murphy, M. K., Okabe, P., Sherrod, R. *Noble Gas Management: SBMOF 1 vs. NUCON Carbon*; PNNL-33314: The U.S. Department of Energy - Office of Nuclear Energy: GAIN VOUCHER, 2022.
13. Sadergaski, L. R., Andrews, H. B., Simultaneous quantification of uranium(VI), samarium, nitric acid, and temperature with combined ensemble learning, laser fluorescence, and Raman scattering for real-time monitoring. *Analyst* **2022**, 147, 4014-4025.
14. Liu, J., Thallapally, P. K., Strachan, D., Metal−Organic Frameworks for Removal of Xe and Kr from Nuclear Fuel Reprocessing Plants. *Langmuir* **2012**, 28, 11594-11589.